IEEE Access Multidisciplinary | Rapid Review | Open Access Journal

Received January 20, 2018, accepted February 25, 2018, date of publication March 2, 2018, date of current version March 28, 2018.

Digital Object Identifier 10.1109/ACCESS.2018.2811679

Modeling and Analysis of One-Tier Ultradense Multiuser Networks

QIAOSHOU LIU[1,2], ZHONGPEI ZHANG[1], HAONAN HU[2,3], AND JIANGPAN SHI[2]

[1]National Key Laboratory of Science and Technology on Communications, University of Electronic Science and Technology of China, Chengdu 611731, China
[2]School of Communication and Information Engineering, Chongqing University of Posts and Telecommunications, Chongqing 400065, China
[3]Department of Electronic and Electrical Engineering, The University of Sheffield, Sheffield S10 2TN, U.K.

Corresponding author: Qiaoshou Liu (liuqs@cqupt.edu.cn)

This work was supported in part by the National Natural Science Foundation of China under Grant 61571003 and Grant 61671128, and in part by the Science and Technology Research Program of the Chongqing Municipal Education Commission under Grant KJ1704095.

ABSTRACT Most research on stochastic geometry has uniformly treated all users in cellular networks. In reality, the performance of a user depends strongly on the distances from a user to the tagged base station and other interfering base stations. Meanwhile, the throughput of a network is decided by the number of base stations and the number of users that can be served in the cell. This paper aims to investigate the achievable performance of users located at different positions in the Voronoi cell. First, we proposed a near formula of distribution of distances from users to their tagged base stations. Then, we deduce the coverage probabilities and ergodic rates of different users in the cell when the network is fully loaded or partially loaded. Finally, we proposed a novel definition of network throughput to respond to the networks' throughput in real time. We compare all our derivations to the Monte Carlo simulation. The numerical results are very close to the simulation results.

INDEX TERMS Coverage probability, stochastic geometry, throughput, Voronoi cell.

I. INTRODUCTION

Thanks to the hardware development of smart devices and the significant efforts of software engineers, we can enjoy high-quality multimedia data services, games (even 3D games) and sharing of large files in real time at any place using portable phones, iPads and various devices through wireless networks. This results in a significant challenge for the capabilities of wireless networks, especially for 4G networks. In fact, the requirement for such capabilities is continually and rapidly growing. Many studies forecast that the capabilities will grow 1000-fold between 2010 and 2020 [1]–[5]. To address this problem, many key technologies, such as Massive MIMO, mm-Wave, and Ultra-Dense Networks (UDN) will be exploited in the forthcoming 5G wireless networks [5]–[8]. Ultra-Dense Networks is a promising technology to cope with the high capability requirements and improve the signal to interference plus noise ratio (SINR) received by mobile users and the space reuse efficiency of the spectrum by deploying more small base stations (SBSs) to reduce the radius of coverage in a given area.

Recently, stochastic geometry has been widely accepted as a powerful mathematical tool for modelling and analysis of wireless networks. Stochastic geometry models of BSs and mobile users conform more closely with reality than regular models such as the hexagonal model and grid model. Reference [9] proposed a method of analysis and design of wireless networks utilizing stochastic geometry and random graphs. Furthermore, [10] analyzed the performance of spatial and opportunistic Aloha networks exploiting Poisson shot noise field theory when the channel is a Rayleigh fading channel. One of the most important contributions to the study of UDN using stochastic geometry can be found in [11], where the author analyzed the one-tier UDN and developed a closed-form expressions of coverage and ergodic rate under specific channels exploiting the spatial Poisson point process (P.P.P.). In [12], a two-tier Heterogeneous Ultra-Dense Network (HUDN) was investigated based on the results of [11]. The total reused spectrum was partitioned to B sub-channels. Each sub-channel served only one user, and only one user could be served by one sub-channel. The author optimized the throughput by adjusting the bias of users and allocations of spectrum between two tiers. Gotsis [13] investigated the effects of different spatial coordination strategies for a multi-user UDN.

In the models of the aforementioned studies and others, each user communicated with its closest BS (small base

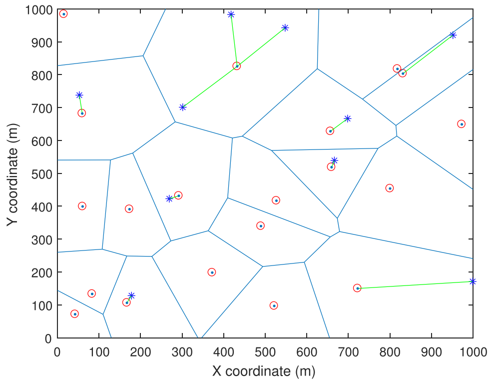

FIGURE 1. 20 SBSs (red circle) and 10 mobile users (blue stars) were randomly deployed in a 1 km^2 area according some homogenous P.P.P.

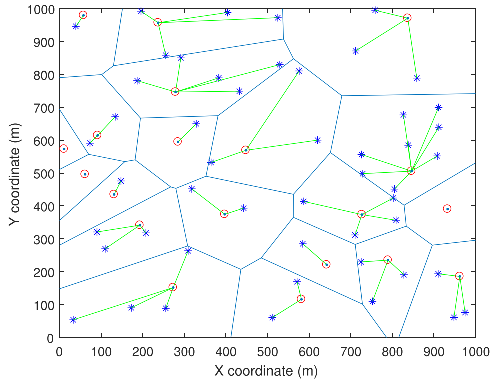

FIGURE 2. 20 SBSs (red circle) and 50 mobile users (blue stars) were randomly deployed in a 1 km^2 area according some homogenous P.P.P.

station or macro base station with bias), and all other BSs acted as interferers. All users in a given cell were treated uniformly; i.e., the coverage probability was the average successful probability of all users in the cell accessing the BS. In this case, the coverage probability does not depend on the density of the BSs. The models of these studies hint that all users can be served by BSs, so the coverage probability does not depend on the density of users. In fact, there would be a significant difference in performance if the coverage probabilities were the same between different networks. Reference [14] exploited the meta distribution of signal to interference ratio (SIR) to analyze the coverage probability and its bound and variance. The meta distribution provides fine-grained information on the SIR and answers questions such as "What fraction of users in a Poisson cellular network achieves 90% link reliability if the required SIR is 5 dB?" [15]. In these two studies, all users can be served, and the performance does not depend on the densities of the BSs and users. Reference [16] analyzed the coverage probabilities based on either a fully or partially loaded network with LOS and NLOS propagation models in a one-tier UDN. The results show that the coverage probabilities depend on both the densities of SBSs and users. However, the coverage probabilities are also the average successful probabilities. The users in the same cell were not analyzed individually.

Practically, the distribution of users has the characteristics of time and region [17]. However, in a UDN, the networks will work with a full load or partial load at different times. Meanwhile, the random deployment of BSs and locations of users complicates the problem.

Fig. 1 and Fig. 2 illustrate two randomly deployed networks comprising SBSs and mobile users in 1 km^2. In Fig. 1, the number of SBSs is greater than the number of users, but there is a Voronoi cell (unless otherwise specified, all cells mentioned in this paper refer to Voronoi cells) that contains more than one mobile user. Fig. 2 shows that most Voronoi cells contain more than one mobile user when the number of users is much greater than the number of SBSs. However, there are several Voronoi Cells that contain one or no users.

As mentioned above, on the one hand, some users cannot access their closest SBSs because the number of users in the cell is greater than the number of users that can be served by the BS. These extra users must communicate with their second or third closest SBSs. On the other hand, some users located at the edge of a cell with high outage must coordinate communication with more than one SBS. It is very important to analyze the performance of different users located at different positions in the cell. This will provide guidance for transferring some users to other SBSs or spatial coordination strategies, which is not within the scope of this paper.

In this paper, we assume that one SBS will serve multiple users by frequency division multiple access (FDMA) in a one-tier UDN. The users will be ordered according to the distances from the users to their tagged SBS (the closest SBS) in a Voronoi cell. The focus of this paper is the successful probabilities of the k^{th} closest users accessing their tagged SBS when either the network is fully or partially loaded. The main contributions of this paper are summarized in the following: (a) We propose a near approach to analyze the distribution of distances from different users to their tagged SBS in a Voronoi cell. We then give the revised probability density function of the distance. (b) We give the closed-form expressions of coverage probabilities and ergodic rates for users located at different positions in the Voronoi cell when the network is fully loaded. We then extend the results when the network is partially loaded. (c) We propose a novel definition of network throughput, which can respond to the throughput of the network in real time.

The remainder of the paper is organized as follows: In Section II, we describe the system model. We show our formulation for calculating the SINR, coverage probability, and ergodic rate in Section III. The throughput of the network is analyzed in Section IV. The numerical results are compared with Monte Carlo simulation results in Section V. Finally, we provide conclusions in Section VI.

II. SYSTEM MODEL

In this paper, we consider a cellular network that consists of densely deployed small base stations and mobile users arranged according to some homogeneous Poisson point process Φ_s and Φ_u with intensity λ_s and λ_u, respectively, in the Euclidean plane; i.e., $\Phi_s \sim PPP(\lambda_s)$, $\Phi_u \sim PPP(\lambda_u)$. The total available frequency spectrum reused by all SBSs has a bandwidth of B Hz and is partitioned into N_c sub-channels. Each mobile user chooses the closest SBS (minimal distance) to communicate and is served by only one sub-channel of its tagged SBS. Each sub-channel services no more than one user; i.e., one SBS can serve no more than N_c users. Assume that there is no interference between different sub-channels due to orthogonality. The interference comes only from the same sub-channels reused in different cells. Each sub-channel operates at a fix power P_s. The numbers of SBSs (N_s), users (N_u), and sub-channels (N_c) satisfy $N_s < N_u < N_s N_c$. This indicates that each small BS must serve more than one of users at most times. In fact, there may be no users or more than N_c users in one cell because of the random locations of users, regardless of the values of N_s and N_u.

When SBSs and users are randomly deployed according to some P.P.P. in cellular networks, it is very easy to obtain the distribution of distances from different users to one SBS or from different SBSs to one user. For notational convenience, we denote SBSs and users by their locations. Without loss of generality, we consider a typical SBS b_o located at the origin. u_k denotes the k^{th} closest user to b_o in the whole network. The random variable (r.v.) R_k denotes the distance from u_k to b_o, where $k = 1, 2, 3, \cdots; k = 1$ means that u_1 is the closest user of b_o; and R_1 is the distance between them. However, this does not mean that b_o is surely the closest SBS of u_1 conversely. All R_k satisfy $R_1 \le R_2 \le R_3 \le \cdots$ (all R_k are ordered by distance). Based on the characteristics of P.P.P., we can easily obtain the cumulative distribution functions (CDF) of distances from the k^{th} closest user in the whole network to the SBS b_o as

$$F_{R_k}(r) = 1 - \sum_{i=1}^{k} \frac{\left(\lambda_u \pi r^2\right)^{i-1}}{(i-1)!} e^{-\lambda_u \pi r^2} \tag{1}$$

The corresponding probability density function (PDF) is as follows:

$$f_{R_k}(r) = \frac{\left(\lambda_u \pi r^2\right)^{k-1}}{(k-1)!} 2\lambda_u \pi r e^{-\lambda_u \pi r^2} \tag{2}$$

Unfortunately, the k^{th} closest user to the SBS in the whole network is not surely the k^{th} closest user to the SBS in the Voronoi cell (VC). In fact, each of the $\left\{(k+i)^{th} : i = 0, 1, 2, \cdots\right\}$ closest users in the whole network may be the k^{th} closest user in the VC, with a probability that decreases with increasing i and the ratio of N_s/N_u. It is very difficult to obtain the distributions of distances from the k^{th} user to the SBS in the VC because of the irregularity of the cell. No works on this subject have appeared in the literature. In this paper, we propose a near approach to address this problem. First, we consider the k^{th} closest user to the SBS in the whole network, while the user is in the VC of the SBS. In this case, we can use this user u_k instead of the k^{th} closest user in the cell of the SBS. This is always satisfied with a very high probability when k is small and N_u/N_s is very large. u_k belongs to the VC of the SBS, which means that $\Phi_s\left(B_{r<R_k}(u_k)\right) = 0$, $\Phi_s(\cdot)$ is the count measure of the SBS. Thus, the CDF of the distance of the closest user in the VC of the SBS can be rewritten from (1) as follows:

$$\begin{aligned} F_{R_k}(r) &= P\{R_k < r\} \\ &= 1 - \sum_{i=1}^{k} \frac{\left(\lambda_u \pi r^2\right)^{i-1}}{(i-1)!} \cdot e^{-\lambda_u \pi r^2} \cdot e^{-\lambda_s \pi r^2} \end{aligned} \tag{3}$$

We can then obtain the PDF as follows:

$$\begin{aligned} f_{R_k}(r) = &\frac{\left(\lambda_u \pi r^2\right)^{k-1}}{(k-1)!} \cdot 2\lambda_u \pi r e^{-\lambda_u \pi r^2} e^{-\lambda_s \pi r^2} \\ &+ \sum_{i=1}^{k} \frac{\left(\lambda_u \pi r^2\right)^{i-1}}{(i-1)!} \cdot 2\lambda_s \pi r e^{-\lambda_s \pi r^2} e^{-\lambda_u \pi r^2} \end{aligned} \tag{4}$$

As mentioned above, we can use u_k instead of the k^{th} closest user in the VC when k is small and N_u/N_s is large. However, there will be a large difference when k is large or N_u/N_s is small because the probability that u_k belongs to the VC and is the k^{th} closest user in the VC begins to decrease. To compensate for this decrease, we revise (4) as follows:

$$F_{R_k}(r) = 1 - \sum_{i=1}^{k} \frac{\left((\lambda_u + \lambda_s)\pi r^2\right)^{i-1}}{(i-1)!} e^{-(\lambda_u+\lambda_s)\pi r^2} \tag{5}$$

Thus, the PDF can be found as

$$f_{R_k}(r) = \frac{\left((\lambda_u + \lambda_s)\pi r^2\right)^{k-1}}{(k-1)!} 2(\lambda_u + \lambda_s)\pi r e^{-(\lambda_u+\lambda_s)\pi r^2} \tag{6}$$

The compensation is intuitive, but the result is perfect. In Section V, we compare the numerical results based on (5) and (6)) with Monte Carlo simulative results. To our surprise, there is only a slight difference between the numerical results and simulative results for any value of k or N_u/N_s. In fact, when a problem cannot be completely solved mathematically, we always solve it by using a near formula first, and then revise it by simulation or some real data if available. The simulations show that our revision is very successful. Fig. 3 illustrates the CDF of distance from the k^{th} user to its tagged SBS when $\lambda_s = 2 \cdot 10^{-5}$ $pieces/m^2$ and $\lambda_u = 4 \cdot 10^{-4}$ $pieces/m^2$.

III. COVERAGE AND RATE

A. COVERAGE PROBABILITY (SUCCESSFUL PROBABILITY OF THE CLOSEST USER ACCESSING ITS TAGGED SBS)

In this paper, we consider only the downlink. For any sub-channel $j \in \{1, 2, 3, \cdots, N_c\}$, the coverage probability of the k^{th} closest user in the cell is defined as

$$p_k(T, \alpha, \lambda_s, \lambda_u) \triangleq \mathbb{P}[SINR > T] \tag{7}$$

Equation (7) indicates that the user can successfully accesses the sub-channel of its tagged SBS for demodulating and decoding if and only if the SINR received is greater than

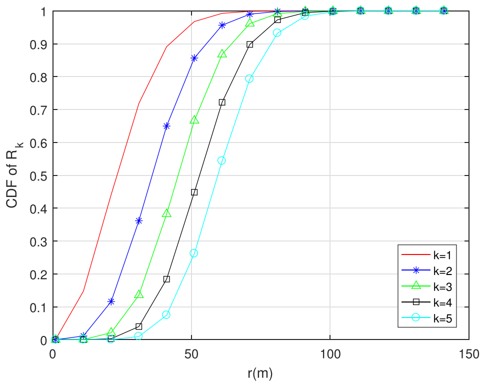

FIGURE 3. CDF of R_k, small base stations and mobile users randomly deployed according to P.P.P.. $\lambda_s = 2 * 10^{-5}$ *pieces*$/m^2$ and $\lambda_u = 4 * 10^{-4}$ *pieces*$/m^2$.

the minimal predefined threshold T. The SINR of the mobile user from its tagged small BS can be expressed as

$$SINR = \frac{hr^{-\alpha}}{\sigma^2 + I_s} \tag{8}$$

where

$$I_s = \sum_{i \in \Phi_s \backslash b_o} g_{s,i} R_{s,i}^{-\alpha}$$

is the cumulative interferences from all sub-channels j of other SBSs (except the tagged SBS for the mobile user at the origin and denoted by b_o). $R_{s,i}$ is the distance from the user to its i^{th} interfering SBS. $g_{s,i}$ is the interference channel coefficient of arbitrary but independent identical distribution for all i. α is the path loss exponent; generally, $\alpha > 4$ outdoors. In a UDN, the noise is always neglected because it is very small, so most of the interference comes from the inter-cell at the same sub-channel [18].

Theorem 1: When neglecting the effect of noise and considering only the interference of other SBSs, the probability that the k^{th} closest mobile user who belongs to the Voronoi cell of SBS b_o successfully accesses any one sub-channel j of small BS b_o is

$$p_k(T, \lambda_s, \lambda_u, \alpha) = \frac{(\lambda_u + \lambda_s)^k}{(\lambda_s(\rho(T,\alpha)+1)+\lambda_u)^k} \tag{9}$$

Proof:

$$\begin{aligned} & p_k(T, \lambda_s, \lambda_u, \alpha) \\ &= \mathbb{E}_r[\mathbb{P}[SINR > T | r]] \\ &= \int_{r>0} \mathbb{P}[SINR > T | r] \cdot f_{R_k}(r)\, dr \\ &= \int_{r>0} \mathbb{P}\left[\frac{P_s h r^{-\alpha}}{\sigma^2 + I_s} > T \middle| r\right] \cdot f_{R_k}(r)\, dr \\ &= \int_{r>0} \mathbb{P}\left[h > \frac{Tr^\alpha}{P_s}\left(\sigma^2 + I_s\right) \middle| r\right] \cdot f_{R_k}(r)\, dr \end{aligned} \tag{10}$$

In this paper, the channels between users and SBSs are independent and experience only Rayleigh fading. Let $h \sim \exp(1)$; we can then obtain

$$\begin{aligned} & \mathbb{P}\left[h > \frac{Tr^\alpha}{P_s}\left(\sigma^2 + I_s\right) \middle| r\right] \\ &= \mathbb{E}_{I_s}\left[\left[h > \frac{Tr^\alpha}{P_s}\left(\sigma^2 + I_s\right) \middle| r, I_s\right]\right] \\ &= \mathbb{E}_{I_s}\left[\exp\left(-\frac{1}{P_s} Tr^\alpha \left(\sigma^2 + I_s\right)\right) \middle| r\right] \\ &= e^{-\frac{1}{P_s}Tr^\alpha \sigma^2} \mathcal{L}_{I_r}\left(\frac{1}{P_s} Tr^\alpha\right) \end{aligned} \tag{11}$$

Using the definition of the Laplace transform of P.P.P. [19] yields

$$\begin{aligned} \mathcal{L}_{I_s}(s) &= \mathbb{E}_{\Phi_s, \{g_{s,i}\}}\left[\prod_{i \in \Phi_s \backslash \{B_o\}} {}_{g_{s,i}}\left[\exp\left(-sP_s g_{s,i} R_{s,i}^{-\alpha}\right)\right]\right] \\ &= \mathbb{E}_{\Phi_s}\left[\prod_{i \in \Phi_s \backslash \{b_o\}} \frac{1}{1 + sP_s R_{s,i}^{-\alpha}}\right] \\ &= \exp\left(-2\pi\lambda_s \int_r^\infty \left(1 - \frac{1}{1 + sP_s v^{-\alpha}}\right) v dv\right) \end{aligned} \tag{12}$$

From (11), $s = \frac{1}{P_s} Tr^a$; thus, we can rewrite (12) as

$$\mathcal{L}_{I_s}\left(\frac{1}{P_s} Tr^\alpha\right) = \exp\left(-2\pi\lambda_s \int_r^\infty \frac{T}{T + (v/r)^\alpha} v dv\right) \tag{13}$$

Let $u = \left(\frac{v}{rT^{2/\alpha}}\right)^2$; rewrite (13) as

$$\mathcal{L}_{I_s}\left(\frac{1}{P_s} Tr^\alpha\right) = \exp\left(-\pi\lambda_s r^2 \rho(T, \alpha)\right) \tag{14}$$

where $\rho(T,\alpha) = T^{2/\alpha} \int_{T^{-2/\alpha}}^\infty \frac{1}{1+u^{\alpha/2}} du$. Combining (14) and (11) with (10), we can obtain (15), as shown at the top of the next page. When neglecting the effect of noise, i.e., $\sigma^2 = 0$, (15) can be simplified as (16), as shown at the top of the next page.

B. ERGODIC RATE OF THE k^{th} USER

Ergodic rate is among the important indicators to evaluate a wireless network. For convenient computation, we compute the mean rate in units of nats/s ($1\ nat = 1/\ln(2) = 1.4427\ bits$); i.e., $\ln(1 + SINR)$. Based on the assumptions and results of theorem 1, we obtain the ergodic rate of user u_k (the k^{th} closest distance to the BS in the cell) as follows:

$$\begin{aligned} & R_k(\lambda_s, \lambda_u, \alpha) \\ &= \mathbb{E}[\ln(1 + SINR)] \\ &= \int_{r>0}\int_{t>0} \mathbb{P}\left[\ln\left(1 + \frac{P_s h r^{-\alpha}}{\sigma^2 + I_s}\right) > t\right] f_{R_k}(r)\, dtdr \\ &= \int_{r>0}\int_{t>0} \mathbb{E}\left[e^{\left(-\frac{r^\alpha}{P_s}(\sigma^2 + I_s)\right)(e^t - 1)}\right] f_{R_k}(r)\, dtdr \\ &\underline{\underline{\sigma^2 = 0}} \int_{t>0} \left(\frac{(\lambda_u + \lambda_s)^k}{(\lambda_s(\rho(e^t - 1, \alpha) + 1) + \lambda_u)^k}\right) dt \end{aligned} \tag{17}$$

$$p_k\left(T,\lambda_s,\lambda_u,\alpha\right)=\mathbb{E}\int_{r>0}\left[h>\frac{Tr^\alpha}{P_s}\left(\sigma^2+I_s\right)\bigg|r\right]\cdot f_{R_k}\left(r\right)dr$$
$$=\int_{r>0}e^{-\frac{c}{P_s}Tr^\alpha\sigma^2}\cdot e^{-\pi\lambda_s r^2\rho(T,\alpha)}\cdot\left(\frac{\left(\left(\lambda_u+\lambda_s\right)\pi r^2\right)^{k-1}}{(k-1)!}\cdot 2\left(\lambda_u+\lambda_s\right)\pi re^{-(\lambda_u+\lambda_s)\pi r^2}\right)dr \tag{15}$$

$$p_k\left(T,\lambda_s,\lambda_u,\alpha\right)=\int_{r>0}e^{-\pi\lambda_s r^2\rho(T,\alpha)}\cdot\left(\frac{\left(\left(\lambda_u+\lambda_s\right)\pi r^2\right)^{k-1}}{(k-1)!}\cdot 2\left(\lambda_u+\lambda_s\right)\pi re^{-(\lambda_u+\lambda_s)\pi r^2}\right)dr$$
$$\underline{\underline{t=\pi r^2}}\int_{t>0}\left(\frac{\left(\lambda_u+\lambda_s\right)^k t^{k-1}}{(k-1)!}\right)\cdot e^{-t(\lambda_s\rho(T,\alpha)+\lambda_u+\lambda_s)}dt$$
$$=\frac{\left(\lambda_u+\lambda_s\right)^k}{\left(\lambda_s\left(\rho\left(T,\alpha\right)+1\right)+\lambda_u\right)^k} \tag{16}$$

The derivation of formula (17) can refer to the proof of theorem 1.

C. PARTIALLY LOADED NETWORK

Usually, especially in UDNs, there are not many users that must be served in a cell; i.e., the number of users in the cell is less than the number of sub-channels. In this case, the sub-channels that are not needed to service users can be turned off to reduce the consumption of power and mitigate the interference. From [20], when the SBSs are deployed according to P.P.P. with density λ_s, the PDF of the area of the VC is expressed as

$$f_S\left(x\right)\approx\frac{3.5^{3.5}}{\Gamma\left(3.5\right)}\lambda_s^{3.5}x^{2.5}e^{-3.5\lambda_s x} \tag{18}$$

When the users are randomly located in the network according to P.P.P. with density λ_u, we can easily obtain the mean of the number of users in one cell as follows:

$$E\left[N_{u,V}\right]=\frac{\lambda_u}{\lambda_s} \tag{19}$$

Assume that the total N_c sub-channels are randomly allocated to the users in the cell. Each sub-channel is active (serves one user) with the following probability:

$$p_a=\begin{cases}1, & \frac{\lambda_u}{\lambda_s}\geq N_c\\ \frac{\lambda_u}{\lambda_s\cdot N_c}, & \frac{\lambda_u}{\lambda_{sc}}<N_c\end{cases} \tag{20}$$

We consider a typical SBS b_o located at the origin. Based on the Reduce Palm Theorem [21], all interfering SBSs $\{\Phi_s/b_o\}$ are still a P.P.P. with density of λ_s. For any sub-channel $j\in 1,2,\cdots,N_c$ of b_o, all interfering SBSs in which sub-channel j is active are a P.P.P. with density of $p_a\cdot\lambda_s$ according to the Thinning P.P.P. Theorem [19]. Turning off sub-channels influences not the distribution of distances between users and their tagged SBS but rather the distribution of distances between users and all interfering SBSs except their tagged SBS. Thus, we use $p_a\cdot\lambda_s$ instead of λ_s in (14) but keep λ_s unchanged in (6). We rewrite (9) as follows:

$$p_k\left(T,\lambda_s,\lambda_u,\alpha\right)=\frac{\left(\lambda_u+\lambda_s\right)^k}{\left(p_a\cdot\lambda_s\cdot\rho\left(T,\alpha\right)+\lambda_s+\lambda_u\right)^k} \tag{21}$$

Similarly, the ergodic rate of the k^{th} user can be rewritten as

$$R_k\left(\lambda_s,\lambda_u,\alpha\right)=\int_{t>0}\left(\frac{\left(\lambda_u+\lambda_s\right)^k}{\left(p_a\cdot\lambda_s\cdot\rho\left(e^t-1,\alpha\right)+\lambda_s+\lambda_u\right)^k}\right)dt \tag{22}$$

$p_a=1$ means the network is fully loaded, and p_k and R_k are increasing functions of λ_u but decreasing functions of λ_s. When the network is fully loaded, the distance from the k^{th} user to its tagged SBS will decrease if the number of users increases but the number of SBSs is fixed. The interfering sources will increase if the number of SBSs increases but the number of users is fixed. $p_a<1$ means the network is partially loaded, and p_k and R_k are decreasing functions of λ_u but increasing functions of λ_s. When the network is partially loaded, the interfering sources will increase if the number of users increases but the number of SBSs is fixed. The interfering sources will decrease if the number of SBSs increases but the number of users is fixed. p_k and R_k will achieve maximal values when $\lambda_u/\lambda_s\cdot N_c=1$ if the number of SBSs is fixed. Conversely, p_k and R_k will achieve minimal values when $\lambda_u/\lambda_s\cdot N_c=1$ if the number of users is fixed.

IV. THROUGHPUT

From the (18), we can obtain the probability that there are $k\in\{0,1,2,\cdots\}$ users in a VC as follows:

$$P\left\{N_{u,V}=k\right\}=\int_0^\infty\frac{\left(\lambda_u x\right)^k}{k!}e^{-\lambda_u x}f_S\left(x\right)dx$$
$$=\frac{\lambda_u^k}{k!}\cdot\frac{\left(3.5\lambda_s\right)^{3.5}}{\Gamma\left(3.5\right)}\cdot\frac{\Gamma\left(k+3.5\right)}{\left(3.5\lambda_s+\lambda_u\right)^{k+3.5}} \tag{23}$$

TABLE 1. Parameters.

Parameter	Description	Value (unit)
p_s	Normalized transmit power	1
λ_s	Density of SBSs	- $(pieces/m^2)$
λ_u	Density of users	- $(pieces/m^2)$
α	Path loss exponent	4
B	Bandwidth	20 (MHz)
N_c	Number of sub-channels	20
S	Area of Network	1 (km^2)

The probability that there are more than $k \in \{0, 1, 2, \cdots\}$ mobile users in a VC is

$$p_{>k} = P\{K > k\} = 1 - \sum_{i=0}^{k} P\{K = i\} \tag{24}$$

When the network is fully loaded, the spectrum allocation strategy has a great impact on network performance. Meanwhile, for Monte Carlo simulation, there are more than N_c users in some cells although $\lambda_u/\lambda_s < N_c$. For simple but perfect performance, we randomly allocate the N_c sub-channels to the N_c closest users when there are more than N_c users in the cell. In addition, we randomly allocate the N_c sub-channels to the users in the cell where there are no more than N_c users. In this case, we define the throughput of the network as follows:

$$\tau_{net} = \sum_{i=1}^{N_s} \sum_{k=1}^{N_c} p_{>k-1} \cdot p_k \cdot \log_2(1+T) \tag{25}$$

[12] defines the throughput of a network in a unit area by $\lambda_u \cdot p \cdot \log_2(1+T)$, where p denotes the coverage probability. However, as mentioned above, p is the average successful probability and cannot accurately respond to the performance of the network. The definition does not consider the situation where the number of users is more than the number of users that can be served; it considers only that the network is fully loaded and that all users can be served. Furthermore, the number of users in different cells varies. Thus, $p_{>k-1} \cdot p_k$ can precisely indicate the number of users that can successfully access its tagged SBS in the cell. Equaption (25) is the throughput of the network in real time (changing with the number of users and SBSs) but not the maximal throughput that can be provided by the network.

V. NUMERICAL RESULTS

Table 1 shows the considered parameters and assumptions for both the numerical results and Monte Carlo simulations.

Fig. 4 illustrates how the coverage probabilities of the k^{th} closest users vary with the predefine SIR thresholds when network is fully loaded, and Fig. 5 illustrates the changes in coverage probabilities when the network is partially loaded. Lines with stars denote the numerical results, and dotted lines with squares denote the Monte Carlo simulation results.

In Fig. 4, $k = 1$ indicates the closest user, and $k = 20$ means that the farthest users can be served in the cell. In Fig. 5, $k = 1$ indicates the closest user, and $k = 10$

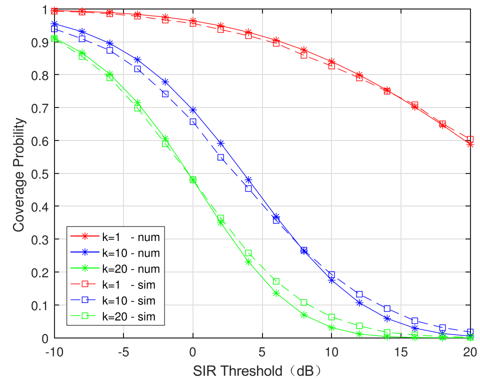

FIGURE 4. Fully loaded network: coverage probabilities change with different SIR thresholds T but fixed $\lambda_s = 2 * 10^{-5}$ $pieces/m^2$ and $\lambda_u = 4 * 10^{-4}$ $pieces/m^2$.

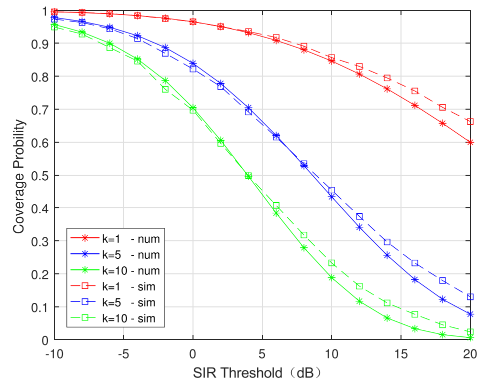

FIGURE 5. Partially loaded network: coverage probabilities change with different SIR thresholds T but fixed $\lambda_s = 2 * 10^{-5}$ $pieces/m^2$ and $\lambda_u = 2 * 10^{-4}$ $pieces/m^2$.

$(\lambda_u/\lambda_s = 10)$ means the farthest users in the cell. There is a slight difference between the numerical results and the Monte Carlo simulation results when the network is fully loaded. The difference increases with increasing SIR threshold when the network is partially loaded as shown in Fig. 5. For Monte Carlo simulation, the numbers of users in each cell are very different, although there are no users in some cells when $\lambda_u/\lambda_s < N_c$; this causes some SBSs to turn off all the sub-channels. Fewer interferers means better performance. As observed in Fig. 4, the farthest users can access their tagged BS with very low probability (less than 0.1 when the SIR threshold is 10 dB), which means they almost cannot communicate with their tagged BS, unless they utilize some joint communication methods. It is very important to know each user's performance to exploit the appropriate strategies in UDN because of the serious interference.

Fig. 6 shows how the coverage probabilities of the k^{th} closest users vary with the number of SBSs when the number of users is fixed. Lines with stars denote the numerical results, and dotted lines with squares denote the Monte Carlo simulation results. The numerical results show that the coverage probabilities decrease with increasing number of SBSs when the network is fully loaded, achieve the minimal value when

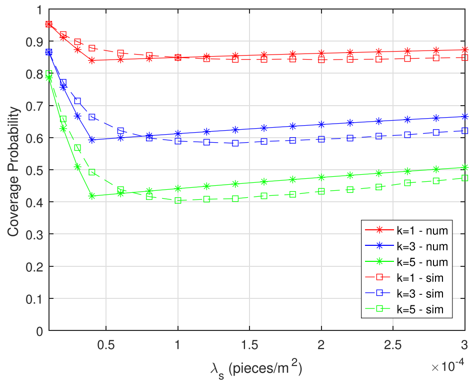

FIGURE 6. **Coverage probabilities at different densities of SBSs, but fixed SIR threshold = 10 dB and $\lambda_u = 8 * 10^{-4}$ *pieces/m*^{2}.**

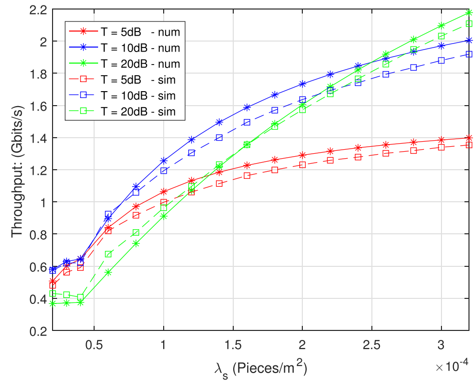

FIGURE 8. **Throughput changes with different densities of SBSs and SIR thresholds but fixed $\lambda_u = 8 * 10^{-4}$ *pieces/m*^{2}.**

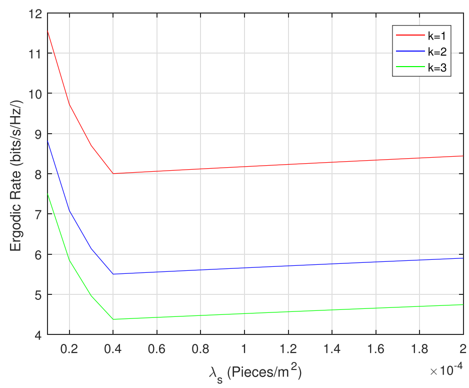

FIGURE 7. **Ergodic Rates at different densities of SBSs, but fixed $\lambda_u = 8 * 10^{-4}$ *pieces/m*^{2}.**

$\lambda_u/\lambda_s = N_c$, and increase with increasing number of SBSs. We force $p_a = 1$ when $\lambda_u/\lambda_s \geq N_c$ in (20) such that the lines of the numerical results sharply turn at the point of $\lambda_u/\lambda_s = N_c$. There is no such limit with the Monte Carlo simulation, so the Monte Carlo simulation results change smoothly and reach the minimal value later but share the same trend as the numerical results. In fact, in Monte Carlo simulation, some cells are occupied by more than N_c users, but others are not when λ_u/λ_s is close to N_c; this is why the Monte Carlo performance is higher than the numerical results at first and then falls below the numerical results.

Fig. 7 illustrates how the ergodic rates of the users vary with the number of SBSs when the number of users is fixed. In fact, the probabilities of coverage and ergodic rates of users have the same trend of change because they have a similar expression as shown in (21) and (22).

As shown in Fig. 6 and Fig. 7, the performance of users will quickly drop with increasing number of SBSs when the network is fully loaded and slowly rise with increasing number of SBSs when the network is partially loaded. This implies, from the users' perspective, that the users who can access their tagged SBSs do not want to increase the number of SBSs to reduce the number of interferers. From the networks' perspective, increasing the number of SBSs will enable more users to access the networks but will sacrifice the interests of some users while increasing fairness. Thus, Fig. 8 shows how the throughput of the whole network changes with the number of SBSs, but the number of users is fixed. Lines with stars denote the numerical results, and dotted lines with squares denote the Monte Carlo simulation results.

As shown in Fig. 8, the throughput will increase with increasing number of SBSs, but the number of users is fixed. The throughput increases slowly when the network is fully loaded with increasing number of SBSs. The throughput increases quickly when the network is partially loaded. Meanwhile, as shown in Fig. 8, the throughput achieves different values at different SIR thresholds T when other parameters are the same. This is because lower T can provide greater coverage probability but will reduce the spectrum efficiency, and vice versa. The larger threshold T can guarantee more throughput when the number of SBSs is larger. However, a relatively small threshold T should be chosen when there are not as many SBSs to achieve better performance.

VI. CONCLUSIONS

In this paper, we have proposed a near approach to formulate the distributions of distances from users located at different positions in a Voronoi cell to their tagged SBS. This will reveal more information about the performance of networks. The numerical results show better performance in coverage probabilities and ergodic rates of users close to their tagged SBS and worse performance of users far from their tagged SBSs. This will guide the design of spatial coordination strategies in our future work.

As the main findings of our work, in a one-tier UDN, the coverage probabilities will drop quickly with increasing number of SBSs when the network is fully loaded. The coverage probabilities will increase slowly with increasing number of SBSs when the network is partially loaded. The throughput of the network increases slowly when the network is fully loaded and increases quickly when the network is partially loaded with increasing number of SBSs.

REFERENCES

[1] Ericsson, "5G radio access, research and vision," Ericsson, Stockholm, Sweden, White Paper, 2013.

[2] I. Hwang, B. Song, and S. S. Soliman, "A holistic view on hyper-dense heterogeneous and small cell networks," *IEEE Commun. Mag.*, vol. 51, no. 6, pp. 20–27, Jun. 2013.

[3] O. Galinina, A. Pyattaev, S. Andreev, M. Dohler, and Y. Koucheryavy, "5G multi-RAT LTE-WiFi ultra-dense small cells: Performance dynamics, architecture, and trends," *IEEE J. Sel. Areas Commun.*, vol. 33, no. 6, pp. 1224–1240, Jun. 2015.

[4] E. Hossain, M. Rasti, H. Tabassum, and A. Abdelnasser, "Evolution toward 5G multi-tier cellular wireless networks: An interference management perspective," *IEEE Wireless Commun.*, vol. 21, no. 3, pp. 118–127, Jun. 2014.

[5] S. Chen and J. Zhao, "The requirements, challenges, and technologies for 5G of terrestrial mobile telecommunication," *IEEE Commun. Mag.*, vol. 52, no. 5, pp. 36–43, May 2014.

[6] A. Alexiou, "Wireless world 2020: Radio interface challenges and technology enablers," *IEEE Veh. Technol. Mag.*, vol. 9, no. 1, pp. 46–53, Mar. 2014.

[7] X. Ge, S. Tu, G. Mao, and C. X. Wang, "5g ultra-dense cellular networks," *IEEE Trans. Wireless Commun.*, vol. 23, no. 1, pp. 72–79, Feb. 2016.

[8] P. Kela, J. Turkka, and M. Costa, "Borderless mobility in 5G outdoor ultra-dense networks," *IEEE Access*, vol. 3, pp. 1462–1476, 2015.

[9] M. Haenggi, J. G. Andrews, F. Baccelli, O. Dousse, and M. Franceschetti, "Stochastic geometry and random graphs for the analysis and design of wireless networks," *IEEE J. Sel. Areas Commun.*, vol. 27, no. 7, pp. 1029–1046, Sep. 2012.

[10] F. Baccelli, B. Blaszczyszyn, and P. Muhlethaler, "Stochastic analysis of spatial and opportunistic Aloha," *IEEE J. Sel. Areas Commun.*, vol. 27, no. 7, pp. 1105–1119, Sep. 2009.

[11] J. G. Andrews, F. Baccelli, and R. K. Ganti, "A tractable approach to coverage and rate in cellular networks," *IEEE Trans. Commun.*, vol. 59, no. 11, pp. 3122–3134, Nov. 2011.

[12] W. C. Cheung, T. Q. S. Quek, and M. Kountouris, "Throughput optimization, spectrum allocation, and access control in two-tier femtocell networks," *IEEE J. Sel. Areas Commun.*, vol. 30, no. 3, pp. 561–574, Apr. 2012.

[13] A. G. Gotsis, S. Stefanatos, and A. Alexiou, "Spatial coordination strategies in future ultra-dense wireless networks," in *Proc. Int. Symp. Wireless Commun. Syst.*, 2014, pp. 801–807.

[14] M. Haenggi, "The meta distribution of the SIR in Poisson bipolar and cellular networks," *IEEE Trans. Wireless Commun.*, vol. 15, no. 4, pp. 2577–2589, Apr. 2016.

[15] Y. Wang, M. Haenggi, and Z. Tan, "The meta distribution of the SIR for cellular networks with power control," *IEEE Trans. Commun.*, to be published.

[16] C. Galiotto *et al.*, "Effect of LOS/NLOS propagation on 5G ultra-dense networks," *Comput. Netw.*, vol. 120, pp. 126–140, Jun. 2017.

[17] S. F. Yunas, M. Valkama, and J. Niemela, "Spectral and energy efficiency of ultra-dense networks under different deployment strategies," *IEEE Commun. Mag.*, vol. 53, no. 1, pp. 90–100, Jan. 2015.

[18] Y. S. Soh, T. Q. S. Quek, M. Kountouris, and H. Shin, "Energy efficient heterogeneous cellular networks," *IEEE J. Sel. Areas Commun.*, vol. 31, no. 5, pp. 840–850, May 2013.

[19] F. Baccelli and B. Bllaszczyszyn, "Possion point process," in *Stochastic Geometry and Wireless Networks: Theory*. New York, NY, USA: Now, 2009, pp. 3–10.

[20] J.-S. Ferenc and Z. Néda, "On the size distribution of Poisson Voronoi cells," *Phys. A, Statist. Mech. Appl.*, vol. 385, no. 2, pp. 518–526, Nov. 2007.

[21] D. Stoyan, W. S. Kendall, and J. Mecke, "Reduced palm distributions," in *Stochastic Geometry and Its Applications*, 3rd. London, U.K.: Wiley, 2013, pp. 131–133.

QIAOSHOU LIU was born in Lüliang, Yunnan, China, in 1979. He received the B.S. and M.S. degrees in communication engineering from the Chongqing University of Posts and Telecommunications, Chongqing, China, in 2002 and 2006, respectively. He is currently pursuing the Ph.D. degree in communication and information with the National Key Laboratory of Science and Technology on Communication, University of Electronic Science and Technology of China, Chengdu, China. He is also an Associate Professor with the School of Information and Communication Engineering, Chongqing University of Posts and Telecommunications. His research interests include interference management, ultra-dense networks, heterogeneous networks, stochastic geometry, and IoT.

ZHONGPEI ZHANG received the Ph.D. degree in traffic information engineering from Southwest Jiaotong University, Chengdu, China, in 2000. From 2001 to 2003, he held a post-doctoral position at Tsinghua University. From 2004 to 2005, he was a Research Scientist with the University of Oulu, Oulu, Finland. He is currently a Professor with the University of Electronic Science and Technology of China. His research interests include wireless communication networks, equalization and iterative receivers, space–time coding, and noncoherent detection algorithms.

HAONAN HU received the B.S. degree in information and communication engineering from the Beijing University of Posts and Telecommunications, China, in 2010, and the M.S. degree in information and communication engineering from the Chongqing University of Posts and Telecommunications, China, in 2013. He is currently pursuing the Ph.D. degree with the Communication Group, Department of Electronic and Electrical Engineering, The University of Sheffield, U.K. He is also a Teaching Assistant with the School of Information and Communication Engineering, Chongqing University of Posts and Telecommunications. His research interests include interference management, heterogeneous networks, LTE-LAA networks, and stochastic geometry.

JIANGPAN SHI is currently pursuing the M.S. degree in information and communication engineering with the Chongqing University of Posts and Telecommunications. Her research interests include ultra-dense networks.